SF2A 2013
L. Cambrésy, F. Martins, E. Nuss and A. Palacios (eds)

ANGULAR MOMENTUM EVOLUTION MODEL FOR SOLAR-LIKE STARS

Florian Gallet[1]

Abstract. We present new models for the rotational evolution of solar-like stars between 1 Myr and 10 Gyr with the aim to reproduce the rotation period distributions observed for star forming regions and young open clusters within this age range. The models include a new wind braking law based on recent numerical simulations of magnetized stellar winds and specific dynamo and mass-loss prescriptions are adopted to link angular momentum loss to angular velocity. The model additionally assume constant angular velocity during the disk accretion phase and allow for decoupling between the radiative core and the convective envelope as soon as the former develops. The models reproduce reasonably well the rotational behaviour of solar-type stars between 1 Myr and the age of the Sun. We conclude that this class of semi-empirical models successfully grasp the main trends of the rotational behaviour of solar-type stars as they evolve and make specific predictions that may serve as a guide for further development.

Keywords: Stars: solar-type, Stars: evolution, Stars: rotation, Stars: mass-loss, Stars: magnetic field

1 Introduction

Simulations of physical events are now essential if we want to understand what happen in the stellar interior and within the stellar environment. These simulations are the only tools we have to test our knowledge and mathematical prescriptions that we use to describe our favourite objects : the stars. There is lots of different fields of physical modelling such as stellar structure, magnetic field and mass-loss rate evolution models. Obviously, the evolution of all these different physical components are somehow link to each other since the structure of the stellar interior will affect the generation of the magnetic field that will in turn affect the quantity of material launched through the stellar winds.

There is few "global" models in the literature that try to combine several isolated physical models. One of these "global" models is the angular momentum evolution that actually rely mainly on the evolution of the stellar interior, magnetic field, and mass-loss rate (e.g., Irwin et al. 2007; Bouvier 2008; Denissenkov et al. 2010; Spada et al. 2011; Reiners & Mohanty 2012). The origin and evolution of stellar angular momentum still remains partly unknown. Recently, new observational constraints on the rotation period distributions of low-mass stars belonging to numerous star forming regions and open clusters, covering an age range from 1 Myr to about 10 Gyr (see, e.g., Irwin & Bouvier 2009; Hartman et al. 2010; Agüeros et al. 2011; Meibom et al. 2011; Irwin et al. 2011; Affer et al. 2012, 2013), have been gained from large photometric surveys. This provides us with the detailed view of how surface rotational velocity changes as the stars evolve from the pre-main sequence (PMS), through the zero-age main sequence (ZAMS) to the late-main sequence (MS). To satisfy observational constraints, most of these models have to incorporate three major physical processes: star-disk interaction during the accretion phase, stellar winds, and redistribution of angular momentum in the stellar interior.

We present here a new angular momentum evolution models for solar-type stars, from 1 Myr to the age of the Sun, that incorporate some of the most recent advances described above and to compare their predictions to the full set of newly available observational constraints. One of the major differences between this study and previous similar studies lies in the wind braking relationship used in the models presented here that relies on recent stellar wind simulations by Matt et al. (2012) and Cranmer & Saar (2011).

[1] UJF-Grenoble 1/CNRS-INSU, Institut de Planétologie et d'Astrophysique de Grenoble (IPAG) UMR 5274, F-38041 Grenoble, France

2 Phenomenological model

2.1 Internal structure

We adopt the Baraffe et al. (1998) NextGen models computed for solar-mass stars of solar metallicity, with a mixing length parameter $\alpha = 1.5$, and helium abundance $Y = 0.275$. Low mass stars are composed of two regions: an inner radiative core and an outer convective envelope. We follow MacGregor & Brenner (1991) by assuming that both the core and the envelope rotate as solid bodies but with different angular velocity. The amount of angular momentum ΔJ to be transferred from the core to the envelope in order to balance their angular velocities is given by

$$\Delta J = \frac{I_{env} J_{core} - I_{core} J_{env}}{I_{core} + I_{env}}, \tag{2.1}$$

where I and J refer to the moment of inertia and angular momentum, respectively, of the radiative core and the convective envelope. As in Allain (1998), we assume that ΔJ is transferred over a constant time-scale τ_{c-e}, which we refer to as the core-envelope coupling timescale.

2.2 Stellar wind

Solar-type stars lose angular momentum as they evolve because of magnetized stellar winds (Schatzman 1962; Weber & Davis 1967). Assuming a spherical outflow, the angular momentum loss rate due to stellar winds can be expressed as

$$\frac{dJ}{dt} \propto \Omega_* \cdot \dot{M}_{wind} \cdot r_A^2, \tag{2.2}$$

where r_A is the averaged value of the Alfvén radius that accounts for the magnetic lever arm, Ω_* is the angular velocity at the stellar surface, and $\dot{M}_{wind}$ is the mass outflow rate. Matt et al. (2012) derived the expression

$$r_A = K_1 \left[\frac{B_p^2 R_*^2}{\dot{M}_{wind} \sqrt{K_2^2 v_{esc}^2 + \Omega_*^2 R_*^2}} \right]^m R_*, \tag{2.3}$$

where $K_1 = 1.30$, $K_2 = 0.0506$, and $m = 0.2177$ are obtained from numerical simulations of a stellar wind flowing along the opened field lines of a dipolar magnetosphere. In Eq. 2.3, R_* is the stellar radius, B_p is the surface strength of the dipole magnetic field at the stellar equator, and $v_{esc} = \sqrt{2GM_*/R_*}$, where M_* is the stellar mass, is the escape velocity. To implement this angular momentum loss rate into our models, we have to express the Alfvénic radius as a function of stellar angular velocity only. We must therefore adopt a dynamo prescription that relates the stellar magnetic field to stellar rotation, as well as a wind prescription that relates the mass-loss rate to the stellar angular velocity. In Eq. 2.3, B_p is the strength of the dipole magnetic field at the stellar equator. Even though the real stellar magnetic field is certainly not a perfect dipole, we identify B_p to the strength of the mean magnetic field $B_* f_*$.

We assume the stellar magnetic field to be dynamo generated, i.e., that the mean surface magnetic field strength scales to some power of the angular velocity. We thus have

$$f_* B_* \propto \Omega_*^b, \tag{2.4}$$

where b is the dynamo exponent, B_* is the strength of the magnetic field, and f_* is the filling factor, i.e., the fraction of the stellar surface that is magnetized (cf. Reiners & Mohanty 2012). Magnetic field measurements suggest that the magnetic field strength B_* is proportional to the equipartition magnetic field strength B_{eq} (see Cranmer & Saar 2011)

$$B_* \approx 1.13 \sqrt{\frac{8\pi \rho_* k_B T_{eff}}{\mu m_H}}, \tag{2.5}$$

with ρ_* the photospheric density, k_B the Boltzmann's constant, T_{eff} the effective temperature, μ the mean atomic weight, and m_H the mass of a hydrogen atom. For the filling factor we used the expression f_{min} from

Cranmer & Saar (2011), but we slightly modified it in order to reproduce the average filling factor of the present Sun ($f_\odot = 0.001$-0.01, see Table 1 of Cranmer & Saar 2011)

$$f_* = \frac{0.55}{\left[1 + (x/0.16)^{2.3}\right]^{1.22}}. \tag{2.6}$$

We used the BOREAS* subroutine, developed by Cranmer & Saar (2011) to get the mean magnetic field $B_* f_*$ as a function of stellar density, effective temperature, and angular velocity. The photospheric density is calculated by BOREAS at the age steps provided by the Baraffe et al. (1998) stellar structure models, and f_* is derived form Eq. 2.6 above. We used the Rossby prescription from Cranmer & Saar (2011), i.e., for a solar-mass star $\tau_{conv} \approx 30$d at 10 Myr, decreasing to 15d at an age ≥ 30 Myr. Measurements of stellar magnetic fields suggest that saturation is reached at $Ro \approx 0.1 - 0.13$ (see Reiners et al. 2009, Fig. 6). With $\tau_{conv} \approx 15$ days, this translates into a dynamo saturation occurring at $\Omega_{sat} \sim 13 - 17\ \Omega_\odot$, which is consistent with the value we derive here. A more detailed description of the model can be found in Gallet & Bouvier (2013).

2.3 Star/disk interaction

For a few Myr during the early pre-main sequence, solar-type stars magnetically interact with their accretion disk. This star-disk magnetic coupling involves complex angular momentum exchange between the components of the system, including the accretion disk, the central star, and possibly both stellar and disk winds. Recently, accretion-powered stellar winds have been proposed as a way to remove from the central star the excess of angular momentum gained from disk accretion (Matt & Pudritz 2005, 2008a,b). However, Zanni & Ferreira (2011) showed that mass and energy supplied by accretion may not be sufficient to provide an efficient spin-down torque by accretion-driven winds. Zanni & Ferreira (2013) proposed that magnetospheric reconnection events occurring between the star and the disk lead to ejection episodes that remove the excess angular momentum. Hence, a free parameter of the models is the accretion disk's lifetime, τ_{disk}, i.e., the duration over which the star/disk interaction occur. After a time τ_{disk}, the star is released from its disk, and is only subjected to angular momentum loss due to magnetized stellar winds (see below). Note that during most of the pre-main sequence, once the disk has been dissipated, angular momentum losses due to magnetized stellar winds are however unable to prevent the star from spinning up as its moment of inertia rapidly decreases towards the ZAMS (cf. Bouvier et al. (1997); Matt & Pudritz (2007); Gallet & Bouvier (2013)). In this model we didn't use any physical star/disk interaction process and the surface angular velocity of the stars is simply held constant during all the disk's lifetime.

3 Angular velocity evolution

The free parameters of the model are the initial rotational period at 1 Myr P_{init}, the core-envelope coupling timescale τ_{c-e}, the disk lifetime τ_{disk}, and the scaling constant of the wind braking law K_1. The value of these parameters are to be derived by comparing the models to the observed rotational evolution of solar-type stars. The models for slow, median, and fast rotators are illustrated in Fig. 1.

For the fast rotator model ($P_{init} = 1.4d$), the disk lifetime is taken to be as short as 2.5 Myr, resulting in a strong PMS spin up. This is required to fit the rapid increase of angular velocity between the youngest clusters at a few Myr ($\Omega_* \simeq 10-20\ \Omega_\odot$) and the 13 Myr h Per Cluster ($\Omega_* \simeq 60\ \Omega_\odot$). The choice of $P_{init} = 1.4$ d for this model is dictated by the fast rotators in the two youngest clusters (ONC and NGC 6530). The core-envelope coupling timescale of the fast rotator model is 12 Myr which is comparable to the 10 Myr coupling timescale adopted by Bouvier (2008), but much longer than the 1 Myr value used in Denissenkov et al. (2010).

The parameters for the median and slow rotator models are quite similar to each other. The initial rotational periods are 7d and 10d for the median and slow rotator models, respectively, as indicated by the rotational distributions of the youngest PMS clusters. For both models we chose a disk lifetime of 5 Myr in order to reproduce the late PMS clusters and the slow rotation rates still observed in the 13 Myr h Per cluster ($\Omega_* \leq 7\ \Omega_\odot$). To account for the weak PMS spin up of the envelope, which leads to moderate velocities on the ZAMS ($\Omega_* \leq 6\ \Omega_\odot$), we had to assume a much longer core-envelope coupling timescale than for fast rotators, namely 28 and 30 Myr for median and slow rotator models, respectively. These values are significantly smaller

*`https://www.cfa.harvard.edu/~scranmer/Data/Mdot2011/`

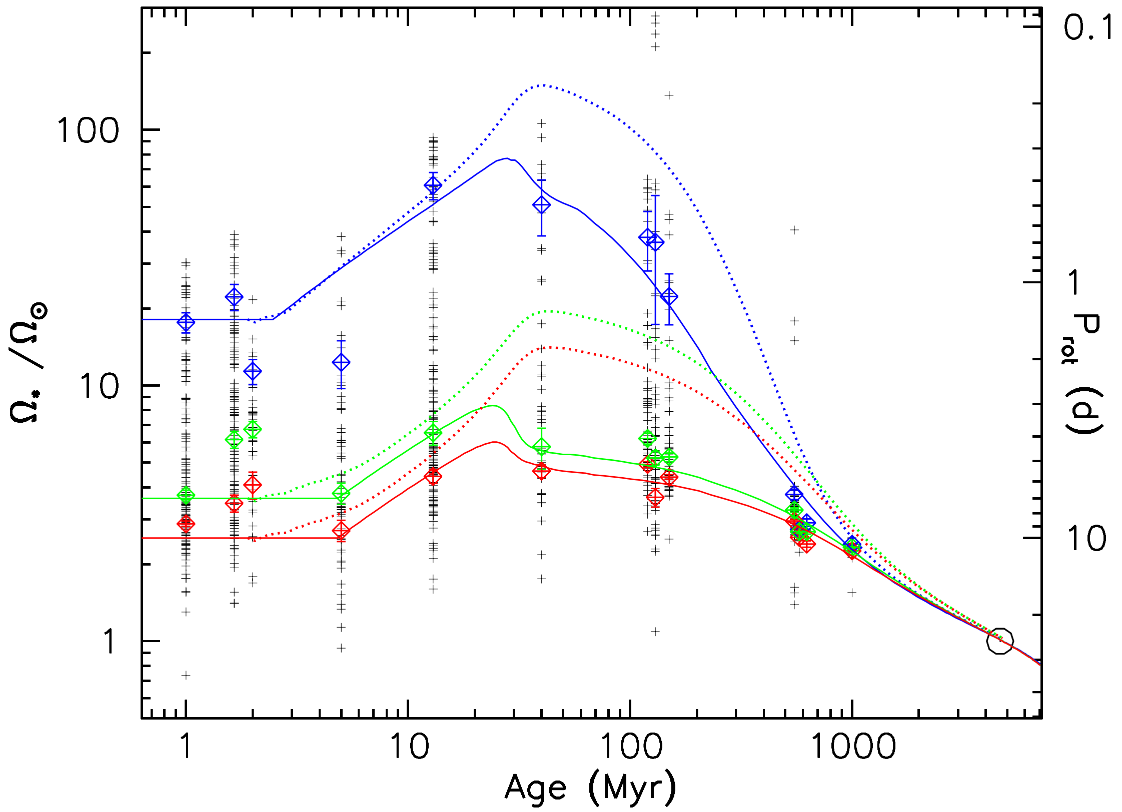

Fig. 1. Angular velocity of the radiative core (dashed lines) and of the convective envelope (solid lines) is shown as a function of time for fast (blue), median (green), and slow (red) rotator models. The angular velocity is scaled to the angular velocity of the present Sun. The blue, red, and green tilted squares and associated error bars represent the 90^{th} percentile, the 25^{th} percentile, and the median, respectively, of the rotational distributions of solar-type stars in star forming regions and young open clusters obtained with a rejection sampling method (see Gallet & Bouvier 2013). The open circle is the angular velocity of the present Sun.

than the 100 Myr coupling timescale derived by Bouvier (2008) and comparable to the value of 55±25 Myr derived by Denissenkov et al. (2010).

By 1 Gyr, the slow, median, and fast rotators models have all converged towards the same surface angular velocity and stars are thereafter braked at a low pace, following Skumanich's relationship (Skumanich 1972), i.e., $\Omega_* \propto t^{-1/2}$. It is quite noticeable, however, that this relationship is not valid earlier on the MS, nor does a unique relationship between age and surface rotation prior to about 1 Gyr for solar-type stars (Epstein & Pinsonneault 2012). All the models presented here yield a complete recoupling between the radiative core and the convective envelope by the age of the Sun, as requested by helioseismology results (Thompson et al. 2003). We emphasize that the evolution of core rotation strongly depends on the core-envelope coupling timescale assumed in the models and currently lacks observational constraints, apart from the solar case.

4 Conclusions

The rotational evolution of solar-type stars can be reasonably well reproduced by the class of phenomenological models presented here. In these models, the physical processes at play are addressed using simplified assumptions that either rely on observational evidence or are based on recent numerical simulations. The fundamental processes such as the generation of surface magnetic fields, stellar mass loss, and angular momentum redistribution, can all be scaled back to the surface angular velocity, which allows us to compute rotational evolution tracks. Pending more physical models still to be developed, these simplified models appear to grasp the main trends of the rotational behavior of solar-type stars between 1 Myr and 4.5 Gyr. The models additionally predict the amount of differential rotation to be expected in stellar interiors. We caution that these predictions are mostly qualitative, as the two-zone model employed here is a crude approximation of actual internal rotational profiles. Also, we show that the evolution of internal rotation as the star ages is quite sensitive to the adopted braking law. In spite of these limitations, one of the major implications of these models is the need to store angular momentum in the stellar core for up to an age of about 1 Gyr. The build-up of a wide dispersion of rotational velocities at ZAMS and its subsequent evolution on the early MS partly reflect this process.

I thank the SF2A organisational committee for this very nice and fruitful week in Montpelier.

References

Affer, L., Micela, G., Favata, F., & Flaccomio, E. 2012, mnras, 424, 11

Affer, L., Micela, G., Favata, F., Flaccomio, E., & Bouvier, J. 2013, ArXiv e-prints

Agüeros, M. A., Covey, K. R., Lemonias, J. J., et al. 2011, apj, 740, 110

Allain, S. 1998, aap, 333, 629

Baraffe, I., Chabrier, G., Allard, F., & Hauschildt, P. H. 1998, aap, 337, 403

Bouvier, J. 2008, aap, 489, L53

Bouvier, J., Forestini, M., & Allain, S. 1997, aap, 326, 1023

Cranmer, S. R. & Saar, S. H. 2011, apj, 741, 54

Denissenkov, P. A., Pinsonneault, M., Terndrup, D. M., & Newsham, G. 2010, apj, 716, 1269

Epstein, C. R. & Pinsonneault, M. H. 2012, ArXiv e-prints

Gallet, F. & Bouvier, J. 2013, aap, 556, A36

Hartman, J. D., Bakos, G. Á., Kovács, G., & Noyes, R. W. 2010, mnras, 408, 475

Irwin, J., Berta, Z. K., Burke, C. J., et al. 2011, apj, 727, 56

Irwin, J. & Bouvier, J. 2009, in IAU Symposium, Vol. 258, IAU Symposium, ed. E. E. Mamajek, D. R. Soderblom, & R. F. G. Wyse, 363–374

Irwin, J., Hodgkin, S., Aigrain, S., et al. 2007, mnras, 377, 741

MacGregor, K. B. & Brenner, M. 1991, apj, 376, 204

Matt, S. & Pudritz, R. E. 2005, apjl, 632, L135

Matt, S. & Pudritz, R. E. 2007, in IAU Symposium, Vol. 243, IAU Symposium, ed. J. Bouvier & I. Appenzeller, 299–306

Matt, S. & Pudritz, R. E. 2008a, apj, 678, 1109

Matt, S. & Pudritz, R. E. 2008b, apj, 681, 391

Matt, S. P., MacGregor, K. B., Pinsonneault, M. H., & Greene, T. P. 2012, apjl, 754, L26

Meibom, S., Barnes, S. A., Latham, D. W., et al. 2011, apjl, 733, L9

Reiners, A., Basri, G., & Browning, M. 2009, apj, 692, 538

Reiners, A. & Mohanty, S. 2012, apj, 746, 43

Schatzman, E. 1962, Annales d'Astrophysique, 25, 18

Skumanich, A. 1972, apj, 171, 565

Spada, F., Lanzafame, A. C., Lanza, A. F., Messina, S., & Collier Cameron, A. 2011, mnras, 416, 447

Thompson, M. J., Christensen-Dalsgaard, J., Miesch, M. S., & Toomre, J. 2003, ARA&A, 41, 599

Weber, E. J. & Davis, Jr., L. 1967, apj, 148, 217

Zanni, C. & Ferreira, J. 2011, apjl, 727, L22+

Zanni, C. & Ferreira, J. 2013, aap, 550, A99